Theoretical Investigation of Doubly Resonant IR−UV Sum-Frequency Vibrational Spectroscopy of Binaphthol Chiral Solution

Ren-hui Zheng,[†,‡] Dong-ming Chen,[†] Wen-mei Wei,[†] Tian-jing He,[†] and Fan-chen Liu*[,†]

Department of Chemical Physics, University of Science and Technology of China, Hefei, Anhui, 230026, P. R. China, Department of Chemistry, Hong Kong University of Science and Technology, Clear Water Bay, Kowloon, Hong Kong, China

Received: October 15, 2005; In Final Form: January 17, 2006

The doubly resonant IR−UV sum-frequency vibrational spectroscopy (SFVS) of 1,1′-bi-2-naphthol (BN) solution and its dispersion spectra are analyzed and computed using the ZINDO//AM1 calculation and the direct approach of Raman scattering tensor calculation, which is based on calculations of Franck−Condon factors and on differentiation of the electronic transition moments with respect to the vibrational normal modes. The calculated results indicate that, for the most intense vibrational bands observed in the SFVS experiment, the calculated frequencies, symmetry, order, intensities, and pattern of the enhanced vibrational modes agree with experiment qualitatively, and due to the Franck−Condon progression, there are the doublet peaks in the corresponding resonant sum-frequency dispersion spectra. The polarization resonance Raman spectra of BN for the vibrational modes appearing in SFVS are also computed and associated with the experiment SFVS of BN. This direct evaluation approach of Raman tensors may provide a way of assigning the doubly resonant IR−UV SFVS.

1. Introduction

Antisymmetric matter tensor is important in connection with antisymmetric scattering and optical activity.[1−6] Recently, antisymmetric transition tensors attracted new interest for a series of studies of optical active sum- and difference-frequency experiments in chiral liquids.[7−10] These spectra yield chiral spectral information about vibrational resonance,[8a] electronic resonances,[9] and double-resonance at both vibrational and electronic resonances,[10] which were reviewed in ref 8b. The theoretical studies indicate that the electric dipole transition is determinant in the UV−IR double-resonant chiral SFG from an isotropic homogeneous system,[11,12] and the scattering amplitude of the UV−IR SFVS can be expressed as the product of the resonant-enhanced anti-Stokes Raman transition polarizabiliy and the IR absorptive transition.[10,13,14]

The compound, 1,1′-bi-2-naphthol (BN), represents popular building blocks for the construction of chiral recognition and chiral catalysts. The interest in BN has increased in the past decade.[10−12,15−17] In quantum chemistry computations of BN, Byers et al., in 1994, presented the observation of the second-harmonic-generation from a BN chiral surface and calculated the hyperpolarizability and chiroptical spectra from monolayers of R−BN using the PPP method, in which only electronic spectrum effects were considered.[15] In 2000, Fischer et al. developed a single-center chiral model and used ab initio calculations to estimate the magnitude of the sum-frequency generation nonlinearity.[7a] In 2003, Fischer et al. also computed the dispersion of the first hyperpolarizability of the optical active solutions by a single excitation configuration interaction method and sum-over-states approach with explicit regard to the Franck−Condon active vibration substructure for all resonant electronic states.[11] In 2001, Setnička et al.[17] calculated and analyzed the vibrational circular dichroism (VCD) spectra of BN by the BPW91/6-31G* density functional theory level. Recently Hayashi et al.[12] performed density functional theory (DFT) calculations combined with a semiempirical molecular orbital method ZINDO/S to determine the energy structure and transition dipole moments of the electronically excited states of BN and calculated the chiral nonlinear optical activity, except the single resonant and doubly resonant IR−UV SFGS. Many quantum computations have been performed to study the behaviors of the surface and bulk second harmonic and sum-frequency generations against the sum-frequency; however, there is no report on the computation analysis of the sum-frequency generation against the IR frequency, i.e., the sum-frequency vibrational spectroscopy (SFVS). On the other hand, even though the electronic absorption spectra, IR, and VCD spectra of BN have been theoretically investigated,[15,17] the resonant Raman (RR) spectra of BN molecules have not been theoretically and experimentally studied and reported yet,[16] which are closely related with the investigation of SFVS of BN. In this paper, we shall compute, analyze, and assign the doubly resonant IR−UV SFVS and polarization resonant Raman spectra of R−BN by quantum chemistry computation using the direct evaluation of the transition moments developed by Warshel et al.[18,19]

In section 2 of this paper, after the bulk nonlinear susceptibilities of the doubly resonant IR−UV SFVS are expressed into the product of the IR transition moment and the resonant-enhanced anti-Stokes Raman polarizability, Warshel et al.'s direct calculation method of resonant Raman tensors is applied to analyze the resonant anti-Stokes Raman polarizabiliy and IR transition moment differentiation with respect to the vibrational normal modes. In sections 3 and 4, based on the above formulas and the ZINDO-1//AM1 computations with the Gaussian 98 package we calculated and assigned the doubly resonant IR−UV SFVS and studied the corresponding resonant sum-

* To whom correspondence should be addressed. E-mail: fcliu@ustc.edu.cn; Fax: +86 551 360 3388.
† University of Science and Technology of China.
‡ Hong Kong University of Science and Technology.

10.1021/jp055901e CCC: $33.50
Published on Web 02/14/2006

frequency dispersion for the R−BN molecule. The results indicate that the calculated ordering and pattern of the enhanced vibrational modes are correct and their intensities agree with the experiment qualitatively; due to the Franck−Condon progression, there are the doublet dispersion peaks. In section 5, the resonant Raman polarization spectra for the vibrational modes appearing in SFVS of BN are computed and studied. This direct evaluation of Raman tensors may provide a method of the assignment of the doubly resonant IR−UV SFVS.

2. Theory

2.1. SFVS Intensity. In electric-dipole approximation the doubly resonant IR−UV sum-frequency vibrational spectroscopy (SFVS) output intensity from a bulk of a chiral medium is given by[10,13,20]

$$I(\upsilon = \upsilon_1 + \upsilon_2) \propto |\chi_B^{(2)}|^2 I_1(\upsilon_1) I_2(\upsilon_2) \quad (1)$$

where $I_1(\upsilon_1)$ is the UV beam intensity at the frequency υ_1, $I_2(\upsilon_2)$ is the IR beam intensity at the frequency υ_2 scanning over vibrational resonances, and $\chi_B^{(2)}$ is the bulk nonlinear susceptibilities. For an isotropic chiral liquid, in terms of first-order molecular hyperpolarizability, orientational averaging yields:[7b,10]

$$\chi_B^{(2)}(\upsilon,\upsilon_2) = \frac{1}{6}\chi_{lmn}^{(2)}(\upsilon,\upsilon_2)\cdot e_{lmn} = \frac{1}{6}\alpha_{\sigma\rho\kappa}^{(2)}\cdot e_{\sigma\rho\kappa} = \frac{N_B}{\epsilon_0}\langle(\hat{l}\cdot\hat{\sigma})\alpha_{\sigma\rho\kappa}^{(2)}(\upsilon,\upsilon_2)(\hat{m}\cdot\hat{\rho})(\hat{n}\cdot\hat{\kappa})\rangle \quad (2)$$

Here e_{lmn} and $e_{\sigma\rho\kappa}$ are the Levi−Civita symbols, $\alpha_{\sigma\rho\kappa}^{(2)}$ is the second-order molecular hyperpolarizability tensor,[21] (l,m,n) and (σ,ρ,κ) refer to the laboratory and molecular coordinates, respectively, and the dot products between the lab and molecule frame are direction cosines. Lorentz local field correction factor is omitted in this paper for simplification. Summation over repeated indices is assumed in eq 2.

In the doubly resonant IR−UV SFVS, when υ_2 is resonant with a particular vibrational transition, the hyperpolarizability $\alpha_{\sigma\rho\kappa}^{(2)}$ can be expressed into the product of the IR transition moment and the resonant-enhanced anti-Stokes Raman polarizability[13,14]

$$\alpha_{\sigma\rho\kappa}^{(2)}(\upsilon,\upsilon_2) = \frac{1}{h^2}\frac{\langle Gg'|\mu_\kappa|Gg\rangle}{(\upsilon_2 - \upsilon_{Gg',Gg} + i\Gamma_{gg'})}\times\sum_{M,m}\left[\frac{\langle Gg|\mu_\sigma|Mm\rangle\langle Mm|\mu_\rho|Gg'\rangle}{(\upsilon - \upsilon_{Mm,Gg} + i\Gamma_{Mm})} - \frac{\langle Gg|\mu_\rho|Mm\rangle\langle Mm|\mu_\sigma|Gg'\rangle}{(\upsilon + \upsilon_{Mm,Gg'} + i\Gamma_{Mm})}\right] \quad (3)$$

where G and M represent ground and excited electronic state, respectively, while g, g', and m represent vibrational levels. μ_σ, μ_ρ, and μ_κ are the dipole moment operators, $\upsilon_{Mm,Gg}$ and $\upsilon_{Mm,Gg'}$ are the frequency differences between the indicated vibronic levels, and Γ_{Mm} is the damping parameter of the Mth electronic state. In the summation of eq 3, both of the electronic excited state M and its vibrational level m are taken into account. From eqs 2 and 3, we obtain[13]

$$\chi_B^{(2)}(\upsilon,\upsilon_2) = \frac{N_B}{6\epsilon_0 h}\frac{\langle Gg'|\vec{\mu}|Gg\rangle}{(\upsilon_2 - \upsilon_{Gg',Gg} + i\Gamma_{Gg'})}\cdot\vec{\alpha}^{ant}(\upsilon) \quad (4)$$

where $[\vec{\alpha}^{ant}(\upsilon)]_\kappa = e_{\kappa\rho\sigma}\alpha_{\rho\sigma}(\upsilon)$ is the antisymmetric part of the anti-Stokes transition polarizability $\alpha_{\rho\sigma}$, which for the vibrational transition $|Gg'\rangle \rightarrow |Gg\rangle$ is given by

$$(\alpha_{\rho\sigma})_{Gg,Gg'} = \frac{1}{h}\sum_{M,m}\left(\frac{\langle Gg|\mu_\rho|Mm\rangle\langle Mm|\mu_\sigma|Gg'\rangle}{(\upsilon - \upsilon_{Mm,Gg} + i\Gamma_{Mm})} - \frac{\langle Gg|\mu_\sigma|Mm\rangle\langle Mm|\mu_\rho|Gg'\rangle}{(\upsilon + \upsilon_{Mm,Gg'} + i\Gamma_{Mm})}\right) \quad (5)$$

In resonant or near resonant cases, eq 5 can be simplified by neglecting its nonresonant part:

$$(\alpha_{\rho\sigma})_{Gg,Gg'} = \frac{1}{h}\sum_{M,m}\frac{\langle Gg|\mu_\rho|Mm\rangle\langle Mm|\mu_\sigma|Gg'\rangle}{(\upsilon - \upsilon_{Mm,Gg} + i\Gamma_{Mm})} \quad (6)$$

2.2. Direct Approach of Calculating Resonant Raman Scattering Tensors.[18] In the following discussion we shall apply the method developed by Warshel and Dauber[18] to analyze the resonant transition polarizability, eq 6, from the electronic wave functions. In 1977, Warshel et al. presented a method for calculations of the complete resonant Raman (RR) vibrational spectrum, which is based on calculations of the Franck−Condon factors and on differentiation of the electronic transition moments with respect to the vibrational normal modes. The reasonability of this method is demonstrated by comparing the evaluation of the RR spectra of β-carotene, β-ionone, and all-trans retinal with the observed relative intensities.[18] The vibronic transition moments in eq 6 can be evaluated by integrating over the electronic coordinates and then expanding the integral in a Taylor series in terms of the molecule normal modes

$$\langle G|\vec{\mu}|M\rangle_Q = \langle G|\vec{\mu}|M\rangle_0 + \sum_t(\partial\langle G|\vec{\mu}|M\rangle/\partial Q_t)_0 Q_t + \cdots \quad (7)$$

Introducing the zero and first-order terms of this expansion into eq 6, replacing Q_t by the dimensionless normal coordinates $\bar{Q}_t = (2\pi c\upsilon/\hbar)^{1/2}Q_t$, and integrating over the vibrational coordinate, it can be obtained

$$(\alpha_{\rho\sigma})_{Gg,Gg'} = A + B \quad (8)$$

where

$$A_{\rho\sigma} = \frac{1}{h}\sum_{Mm}\left\{\frac{\langle G|\mu_\rho|M\rangle_0\langle M|\mu_\sigma|G\rangle_0}{\upsilon_0 - \upsilon_{Mm,Gg} + i\Gamma_{Mm}}\bar{C}(g,m)\bar{C}(g',m)\right\} \quad (9)$$

$$B_{\rho\sigma} = \frac{1}{h}\sum_{Mm}\frac{1}{\upsilon_0 - \upsilon_{Mm,Gg} + i\Gamma_{Mm}}[\langle G|\mu_\rho|M\rangle_0(\partial\langle M|\mu_\sigma|G\rangle/\partial Q_t)_0\bar{C}(g',m)\bar{C}^t(g,m) + \langle G|\mu_\sigma|M\rangle_0(\partial\langle M|\mu_\rho|G\rangle/\partial Q_t)_0\bar{C}(g,m)\bar{C}^t(g',m)] \quad (10)$$

In this paper, the index order of the tensor components is as same as refs 10 and 11 and different from ref 18. In eqs 9 and 10 the summation for the normal modes Q_t is impliedly included. Here $\bar{C}(g,m)$, $\bar{C}(g',m)$, $\bar{C}^t(g,m)$, and $\bar{C}^t(g',m)$ are the vibrational integrals $\langle g,m\rangle$, $\langle g',m\rangle$, $\langle g'|\bar{Q}_t|m\rangle$, and $\langle g|\bar{Q}_t|m\rangle$, respectively. Using the recursion relation (see eqs 9 and 10 in ref 18 and eqs I and II in ref 28) for the vibrational overlap integral, only considering $m_t = 0$ and $m_t = 1$ contributions for Q_t mode, and assuming that there is no difference of vibrational wavenumber between the ground state and excited states but a displacement Δ_t of the potential energy minimum along the normal coordinate Q_t and $\Delta_t \ll 1$. From ref 28 we obtain Franck−Condon factors $\bar{C}(0_t,0_t) \approx \bar{C}(1_t,1_t) = a$, $\bar{C}(0_t,1_t) \approx -\bar{C}(1_t,0_t) \approx -\bar{C}(2_t,1_t)/\sqrt{2} = b$, and $\sqrt{2}\bar{C}(0_t,0_t)\bar{C}(2_t,0_t) \approx -b^2$. Thus, eqs 9 and 10 for the

fundamental anti-Stokes Raman transitions ($g = 0$ and $g' = 1$) are, respectively,[18] Equation 12 indicates that the expression of

$$A_{\rho\sigma} = \sum_M \frac{ab\langle G|\mu_\rho|M\rangle_0\langle M|\mu_\sigma|G\rangle_0}{h}\left\{\frac{1}{\Delta\upsilon_0 + \upsilon_t + i\Gamma_M} - \frac{1}{\Delta\upsilon_0 + i\Gamma_M}\right\} \quad (11)$$

$$B_{\rho\sigma} = \frac{1}{\sqrt{2}h}\sum_M\left[\frac{1}{\Delta\upsilon_0 + i\Gamma_M}\{b^2\langle G|\mu_\rho|M\rangle(\partial\langle M|\mu_\sigma|G\rangle/\partial Q_t)_0 + (a^2 - b^2)\langle G|\mu_\sigma|M\rangle_0(\partial\langle M|\mu_\rho|G\rangle/\partial Q_t)_0\} + \frac{1}{\Delta\upsilon_0 + \upsilon_t + i\Gamma_M}\{a^2\langle G|\mu_\rho|M\rangle(\partial\langle M|\mu_\sigma|G\rangle/\partial Q_t)_0 - b^2\langle G|\mu_\sigma|M\rangle_0(\partial\langle M|\mu_\rho|G\rangle/\partial Q_t)_0\}\right] \quad (12)$$

B term is not symmetric with respect to exchange of the ρ and σ components, under some conditions it might lead to antisymmetric transition polarizabilities and anomalous polarization effects.[18,22] Warshel et al.'s direct method has been applied to the study of the anomalous polarization effect in the resonant Raman spectra of metalloporphyrins, which gives good agreement with the observed depolarization ratio and its dependence on the excitation energy.[22] Ref 18 evaluates the electronic transition moments and their derivative with respect to normal coordinates in the following straightforward way: when the change in the configuration interaction mixing upon displacement from $\vec{r}$, and the integrals $\langle\lambda_i|x|\lambda_{i'}\rangle$ for $i \neq i'$ are neglected, the electronic transition moment can be expressed into

$$\bar{\mu}_\rho^{GM}(\vec{r}) = \sum_{n,i}\sqrt{2}C_n^M\upsilon_{n1i}\upsilon_{n2i}\langle\lambda_i|e\sum_k(\vec{x}_k)_\rho|\lambda_i\rangle = \sum_i q_i^{GM}r_{i\rho} \quad (13)$$

where $\vec{x}$ are the electronic coordinates, λ_i are the Löwdin orthogonalized atomic orbitals, coefficients C_n^M are the components of the Mth eigenvector of the configuration interaction matrix, and q_i^{GM} are the transition monopoles, which are defined as $q_i^{GM} = \Sigma_n\sqrt{2}C_n^M\upsilon_{n1i}\upsilon_{n2i}$, where υ_{ni} is the coefficient of the atomic orbital λ_i in the molecular orbital n. The normal mode vector $\mathscr{R}_s$ defines the transformation between the Cartesian coordinates and normal coordinates

$$\mathrm{M}^{1/2}\delta r = \mathscr{R}^M Q^M \quad (14)$$

where M is a diagonal matrix of the atomic masses. The complete set of vibrational frequencies and the normal coordinates vectors, $\mathscr{R}^M$, can be evaluated by diagonalizing the matrix of mass scaled Cartesian second derivatives of the total potential at the calculated minimum. Equation 13 is differentiated with respect to normal coordinates while holding q_i^{GM} constant:[18]

$$(\partial\mu_\rho^{GM}/\partial Q_t)_0 = (\hbar/2\pi c\upsilon_t)^{1/2}\sum_i q_i^{GM}\mathscr{R}_t^{i\rho}m_i^{-1/2} \quad (15)$$

For a R−BN molecule belonging to C_2 point group, all of its electronic states and vibration states are nondegenerate and their representations are real, thus A term in eq 11 for a BN molecule is symmetric, using time-reversal arguments,[23,24] i.e., $A_{\rho\sigma} = A_{\sigma\rho}$. Hence, using eq 8, eq 4 can be expressed into

$$\chi^{(2)}_{chiral}(\upsilon,\upsilon_2) = \frac{N_B}{6\epsilon_0}\frac{1}{h(\upsilon_2 - \upsilon_{Gg',Gg} + i\Gamma_{Gg'})}\left[\frac{\partial\mu_z}{\partial Q_t}(B_{xy} - B_{yx}) + \frac{\partial\mu_y}{\partial Q_t}(B_{zx} - B_{xz}) + \frac{\partial\mu_x}{\partial Q_t}(B_{yz} - B_{zy})\right] \quad (16)$$

where the derivatives of the IR transition dipole moment with respect to the normal modes of vibration are[25]

$$\frac{\partial\mu_\kappa}{\partial Q_t} = \langle Gg'|\mu_\kappa|Gg\rangle_{Qt} = \langle g'|\langle G|\mu_\kappa|G\rangle|g\rangle_{Qt} = \langle g'|g\rangle\langle G|\mu_\kappa|G\rangle_0 + (\partial\langle G|\mu_\kappa|G\rangle/\partial Q_t)_0\langle g'|Q_t|g\rangle + \cdots = \frac{1}{\sqrt{2}}(\partial\langle G|\mu_\kappa|G\rangle/\partial Q_t)_0. \quad (17)$$

It is known that using the Gaussian software[26] the values of the derivatives of the dipole moments with respect to the Cartesian coordinate $\partial\langle G|\mu_\kappa|G\rangle/\partial p_i$ (κ,$p_i = x,y,z$) can be calculated and saved in the check file when one computes the IR absorption intensities for the vibration modes. From the transformation relation between Cartesian coordinates and normal coordinates, eq 14, we can obtain

$$\frac{\partial\mu_\kappa}{\partial Q_t} = \frac{1}{\sqrt{2}}\sum_i(\partial\mu_\kappa/\partial p_i)_0\mathscr{R}_t^{i\kappa}m_i^{-1/2} \quad (18)$$

Using eqs 16, 12, 18, and 15, the detailed expression $\chi^{(2)}_{chiral}(\omega,\omega_2)$ can be obtained.

3. Computation of Spectral Properties of BN

3.1. Frequency, Intensity, and Symmetry of the Vibrational Bands in UV−IR SFVS, IR, SERS, and VCD Spectra of BN. Applying the BPW91/6-31G** and B3LYP/6-31G** density functional theory method, and the AM1 method with Gaussian 98 program[26], we optimize the structure and calculate and assign the fundamental frequencies and intensities of the vibrational bands in the SFVS,[10] VCD,[17] solid IR, and Raman[16] spectra. The results are shown in Table 1 and are associated with the relative experiments or the other computed results in the literature.

In Table 1 the frequencies computed by the B3LYP/6-31G** density functional are scaled by a factor 0.9614[27] and those by the AM1 method are scaled by a factor 0.868 instead of 0.9532, as recommended by ref 27. Just as pointed out in ref 27, The large percentages (33%) of the total number of frequencies computed by AM1, after scaling by 0.9532, have an error outside the target accuracy (10%). We find that, after scaling by the factor 0.868, the symmetry, the frequencies, and IR intensities of the vibration bands calculated by AM1 fit well with the experiments and the other density functional computations in the literature (see Table 1).

Structural studies and quantum chemical computations of 1,1′-bi-2-naphthol predict that 2-naphthol (2HN) groups are quasi-orthogonal.[16,17,19,27] Due to the steric hindrance of OH group and hydrogen bonds in BN solution,[17] we consider BN as a rigid molecule, and do not make the averages for the dihedral angle between two aromatic planes for dependent properties. The BPW91/6-31G** density functional calculations find a dihedral angle $\theta \approx 86°$ of the two 2-naphthol groups for the R−BN,[17] $\theta \approx 89°$ in computations with with B3LYP/6-31G* density functional, and $\theta \approx 85°$ with semiempirical AM1 Hamiltonian.[11] This suggests that there is likely to be only weak coupling between two naphthol rings, which result in the small

TABLE 1: Calculated Fundamental Frequencies (in cm^{-1}) and IR Intensities of the R−BN Molecule and the Assignment to the IR−UV SFVS Double Resonant, VCD, IR, and Raman Experiments

band	SFG[a]	VCD[b]	IR (solid)[c]	Raman[c] solid (1064 nm)	BPW91 /6-31G**	B3LYP /6-31G*[d]	AM1[e]	band	SFG[a]	VCD[b]	IR (solid)[c]	Raman[c] solid (1064 nm)	BPW91 /6-31G**	B3LYP /6-31G*[d]
1	1335 m	1344 B	1347 s		1353 B (61.6)	1332 B (101.9)	1286 B (40.0)	4	1430 m	1430 B	1435 m	1440 (3)	1435 B (22.6)	1423 B (28.6)
					1363 A (32.4)	1335 A (55.8)	1317 A (2.5)			1439 A			1438 A (17.8)	1426 A (20.3)
2	1355 m				1385 B (5.4)	1356 B (0.92)	1318 B (21.9)	5	1460 m	1464 B	1461 s	1466 sh	1473 B (2.7)	1462 B (2.50)
					1390 A (0.26)	1361 A (0.017)	1350 A (5.1)	6	1484 m	1478 A	1470 s	1473 (2)	1481 A (9.9)	1469 A (8.56)
3	1375 vs	1383 B	1381 vs	1381 (10)	1400 B (25.8)	1376 B (12.4)	1381 B (98.4)	7	1516 s	1504 B	1510 s	1519 (1)	1517 B (47.8)	1503 B (49.5)
		1403 A			1407 A (2.2)	1390 A (0.028)	1383 A (122.4)			1514 A			1520 A (43.2)	1505 A (42.1)

[a] The experimental values from Figure 2 of ref 10. [b] The experimental values from ref 17. [c] The experimental values from ref 16. [d] The calculated frequencies scaled by a factor 0.9614. Two lines correspond to the two components in a VCD band, respectively. m, s, vs, and the number values in the parentheses represent relative intensities of the vibrational bands in Raman, IR, and (DR) IR−UV SFVS spectra. [e] The calculated frequencies scaled by a factor 0.868. Two lines correspond to the two components in a VCD band, respectively.

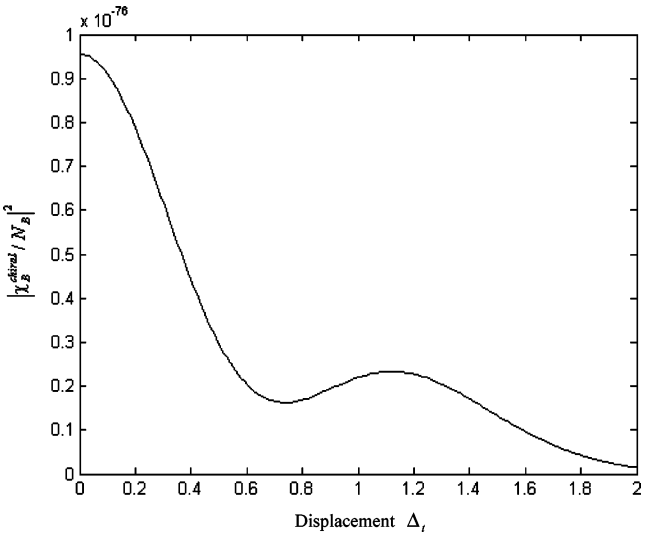

Figure 1. Calculated peak strengths of the chiral spectra $|\chi_B^{chiral}/N_B|^2$ ($(m^4/V)^2$) for vibrational mode of BN at 1383A cm^{-1} versus the displacement Δ_t. The computations of $|\chi_B^{chiral}/N_B|^2$ use ZINDO//AM1 method with SF at 3.8576 eV resonant to the first two excited electronic states.

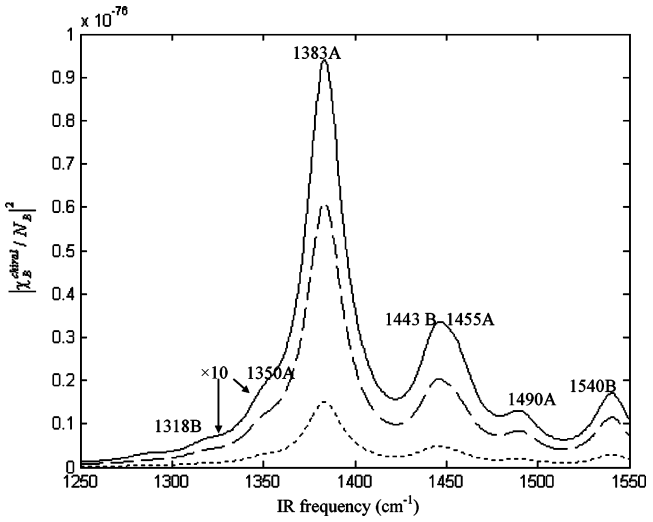

Figure 2. Calculated chiral spectra $|\chi_B^{chiral}/N_B|^2$ ($(m^4/V)^2$) for vibrational modes of R−BN at the range 1250 cm^{-1}−1550 cm^{-1} with SF respectively at 3.8576 eV (solid line), 3.8076 eV (dashed line) and 3.7476 eV (dotted line) resonant to the first two excited states. The computations are based on ZINDO-1//AM1 computations when all the displacements Δ_t are taken to be 0.1. The chiral spectra for vibrational modes at 1318 and 1350 cm^{-1} are multiplied by a factor of 10.

splittings of vibrational bands. However, the doubly resonant IR−UV sum-frequency vibrational spectroscopy of R−BN in Figure 2 of ref 10 shows the line width of chiral spectra is more than 20 cm^{-1}, and the splittings of vibrational frequencies for A and B symmetric bands, due to two naphthol rings coupling, are generally smaller than the chiral spectra line width. For example, the splitting of the bands 3 (1381B and 1383A) is only 2 cm^{-1} computed by the AM1 method, which correspond to the 1375 band of the experiment chiral spectra[10] with about 24 cm^{-1} line width. It is hard to make sure the symmetry of the vibrational bands for the IR−UV double-resonant chiral spectra only according to the frequency computation results. We also calculate the peak strength of the chiral spectra (see Table 4 and Section 4.1) which is useful for assignments of the bands in the chiral spectra. But the symmetry assignments of the bands in SFVS spectra (Figure 2) are temporary.

3.2. Excited Electronic State Levels, Oscillator Strengths, and Transition Moments. We have used ZINDO-1 and TDDFT//B3LYP/6-31G* methods to compute the excited electronic state levels, the transition moments from the ground state to the excited states, and the corresponding oscillator strengths of a BN molecule. The calculated results are listed in Tables 2 and 3, which are associated with the experiments.

The ZINDO procedure has been used to calculate spectroscopic properties of organicπ−electron chromophore.[29] For an AM1 optimized geometry of R−BN, a ZINDO-1 computation in Gaussian 98[26] locates the first two excited singlet states at 3.8276 eV (with oscillator strength $f = 0.0544$) and 3.8444 eV (with $f = 0.0060$), respectively. The lowest two singlet states of BN are split by 136 cm^{-1}. Also, in Table 3, TDDFT//B3LYP/6-31G* method is applied to model the R−BN molecule, and the first two excited states are located 3.8774 and 3.8811 eV, respectively, the corresponding splitting of which is 29.8 cm^{-1}. The excitation energies of first two excited singlet states by ZINDO-1//AM1 agree well with those by TD//B3LYP/6-31G*, and about 0.1 eV larger than the observed first excited absorption peak at 3.70 eV;[15] moreover, the corresponding oscillator strengths agree with the experiment value 0.086[15] (also see Table 2). Thus the ZINDO-1//AM1 method can be applied to analyze doubly resonant IR−UV SFVS of BN when the sum-frequency

TABLE 2: Calculated Excited Electronic States, Oscillator Strengths, and Transition Moments in a.u. for R−BN Using ZINDO Method Based on AM1 Optimization

state	υ (eV)	v (obs)[a]	f(calc)	f(obs)[a]	$\langle i\|x\|0\rangle$	$\langle i\|y\|0\rangle$	$\langle i\|z\|0\rangle$
1 (B)	3.8276	3.7	0.0544	0.086	−0.1021	−0.7551	0.0000
2 (A)	3.8444		0.0060		0.0000	0.0000	0.2533
3 (B)	4.3131	4.5	0.3852	0.216	−0.7487	1.7565	0.0000
4 (A)	4.4392		0.0545		0.0000	0.0000	0.7080
5 (A)	4.4886		0.0008		0.0000	0.0000	0.0860
6 (B)	4.4958		0.0139		−0.2565	0.2449	0.0000
7 (B)	5.1995		0.0731		−0.5597	−0.5105	0.0000
8 (A)	5.2161		0.0276		0.0000	0.0000	0.4650

[a] Data from ref 15.

TABLE 3: Calculated Excited Electronic States, Oscillator Strengths, and Transition Moments in A.U. for R−BN Using TDDFT Method Based on B3LYP/ 6-31G* Optimization

state	v(eV)	v (obs)[a]	f(calc)	f(obs)[a]	$\langle i\|x\|0\rangle$	$\langle i\|y\|0\rangle$	$\langle i\|z\|0\rangle$
1 (B)	3.8774	3.7	0.0073	0.086	−0.0223	0.2758	0.0000
2 (A)	3.8811		0.0001		0.0000	0.0000	−0.0315
3 (B)	4.0576		0.1629		−0.4549	1.1964	0.0000
4 (A)	4.1161		0.0124		0.0000	0.0000	0.3508
5 (A)	4.5168	4.5	0.0332	0.216	0.0215	−0.5473	0.0000
6 (B)	4.5294		0.0000		0.0000	0.0000	0.0015
7 (B)	4.7788		0.0018		−0.0244	0.1216	0.0000
8 (A)	4.7797		0.0004		0.0000	0.0000	−0.0558

[a] Data from ref 15.

TABLE 4: Computed Peak Strengths of the Chiral Spectra $|\chi_B^{chiral}/N_B|^2$ (in the Unit of 1.0×10^{-76} (m^4/V^2)) for Vibrational Modes of R−BN Due to the First Singlet Excited State ^{1}B, the Second Singlet Excited State ^{1}A, and the First Two Singlet Excited State, Respectively, with SF at 3.8576 eV Based on ZINDO-1//AM1 Computations with $\Delta_t = 0.1$

band/$\|\chi_B^{chiral}/N_B\|^2$	^{1}B	^{1}A	^{1}B and ^{1}A
1286 B	3.8×10^{-3}	7.3×10^{-3}	9.9×10^{-4}
1317 A	4.4×10^{-4}	$1.3 \times$ e-10^{-27}	4.4×10^{-4}
1318 B	2.2×10^{-4}	6.9×10^{-4}	1.6×10^{-3}
1350 A	7.4×10^{-3}	6.0×10^{-31}	7.4×10^{-3}
1381 B	1.4×10^{-4}	1.2×10^{-3}	5.3×10^{-4}
1383 A	0.91	2.2×10^{-28}	0.91
1401 B	4.5×10^{-3}	3.7×10^{-2}	1.7×10^{-2}
1403 A	7.1×10^{-3}	3.5×10^{-28}	7.1×10^{-3}
1443 B	0.13	1.0×10^{-2}	0.22
1455 A	0.14	2.3×10^{-30}	0.14
1476 B	2.7×10^{-2}	2.0×10^{-2}	2.2×10^{-3}
1490 A	8.0×10^{-2}	1.5×10^{-29}	8.0×10^{-2}
1540 B	0.16	2.1×10^{-6}	0.16

is resonant with the transition between the ground state and the first two excited states.

4. Computation of $\chi^{(2)}_{chiral}(\upsilon,\upsilon_2)$ for R−BN

4.1. Theoretical SFVS Spectra of BN Molecules. Based on the ZINDO-1//AM1 results and using eqs 16, 12, 15, and 18, we calculate the double-resonant IR−UV SFVS chiral spectra $|\chi_B^{chiral}/N_B|^2$ for vibrational modes of R−BN at the range of 1250 cm^{-1}−1550 cm^{-1}, with SF at 3.8576, 3.8076, and 3.7476 eV, respectively (resonant to the first two singlet excited states), and the calculated results are plotted in Figure 2. Also, the peak strengths of the chiral spectra due to the first singlet excited state ^{1}B, the second singlet excited state ^{1}A, and the first two singlet excited state, respectively, with SF at 3.8576 eV are listed in Table 4. From Figure 2, we see that the position, symmetry, and relative intensity of vibrationl bands in SFVS respectively are 1318 B cm^{-1} (w), 1350 A cm^{-1} (w), 1383A cm^{-1} (vs), 1443 B cm^{-1} (m), 1455 A cm^{-1} (m), 1490 A cm^{-1} (m), and 1540 B cm^{-1} (m). Table 1 shows that the experimental bands and intensity, respectively, are 1335 (m), 1355 (m), 1375 (vs), 1430 (m), 1460 (m), 1484 (m), and 1516 (s). Comparing the calculated chiral spectra with the experimental one, we find that the calculated order and pattern of the vibrational bands in SFVS are correct and their intensities agree with the experiment qualitatively, though the computed peak strength of chiral spectra $|\chi_B^{chiral}/N_B|^2$ for the 1318 and 1350 cm^{-1} vibrational modes are less than the corresponding experimental values by more than 1 order of magnitude. Thus this computation may provide a method of detailed assignment of the double-resonant IR−UV SFVS. Also from Figure 2, we can see that when the sum-frequency is 3.8076 eV, that is 0.05 eV smaller than 3.8576 eV, the corresponding peak strengths of chiral spectra reduce to about one-third of those for the 3.8076 eV cases; when the sum-frequency is 3.7476 eV, those reduce to about one tenth. This trend is in agreement with the experiment[10] and indicates that the chiral spectra depend sensitively on the sum-frequency that greatly enhances the chiral spectra. From Table 4, it is shown that the peak strength of vibrationl band 1383 A cm^{-1} from the first singlet excited state ^{1}B are dominate and about 10^{28} larger than that from the second singlet excited state ^{1}A resonance. This conclusion can also be drawn for the other vibrational bands marked in Figure 2, except the 1318 B cm^{-1} band because the contributions of this band from the first two excited states are of the same order of magnitude. These results indicate that the ^{1}B vibronic states of the BN molecule is particularly important for the chiral SFVS with SF at 3.8576 eV.

Now we describe some detail in the computation of SFVS of BN. First, we need to calculate some parameters in eqs 10, 14, 15, and 17, such as υ_{ni}, R_t, C_n^m, Δ_t, and so on. Molecular orbital coefficients υ_{ni} in eq 13 are obtained using the population analysis after AM1 structural optimization. The Hessian matrix of force constants are saved in the check file when the IR frequency computations are performed, thus, using eq 14, the normal mode vector $\mathscr{R}_s$ defines the transformation between Cartesian coordinates and normal coordinates and can be obtained when diagonalizing the Hessian matrix of force constants scaled by the matrix of mass. When the electric dipole transition moments are computed and shown in Table 2, the configuration interaction coefficients C_n^M are obtained as 0.287 (50 → 54) for the singlet one electron excitation from the molecular orbit ϕ_{n1} ($n1 = 50$) to molecular orbit ϕ_{n2} ($n2 = 54$), for other one electron excitation C_n^M are −0.269 (51 → 55), −0.101 (51 → 56), −0.135 (52 → 54), 0.356 (52 → 57), −0.224 (53 → 55), and 0.353 (53→56) for the first singlet excited state ^{1}B; similarly, C_n^M are 0.290 (50 → 55), −0.308 (51 → 54), −0.130 (52 → 55), 0.370 (52 → 56), 0.155 (53 → 54), and 0.345 (53 → 57) for the second singlet excited state ^{1}A. From the linear absorption spectrum of BN,[9,15] the UV line widths are taken into 1000 cm^{-1}, i.e., $\Gamma_{Mm} = 500$ cm^{-1}.

To calculate the Frank−Cotton factors a, b in eq 12, we apply the related formulas in ref 28 and the suitable displacement parameter Δ_t of the potential minimum of the excited states. To choose a suitable displacement Δ_t, we calculate peak strengths of the chiral spectra $|\chi_B^{chiral}/N_B|^2$ for vibrational mode of R−BN at 1383A cm^{-1} and sketch the curve of $|\chi_B^{chiral}/N_B|^2$ versus displacement Δ_t with SF at 3.8576 eV (resonant to the first two excited states) which is shown in Figure 1. Figure 1 shows that when the displacement Δ_t is taken into 0.1 for 1383A cm^{-1} mode, the corresponding computed peak strength is 0.91 $\times 10^{-76}$ (m^4/V)^2 in good agreement with the experimental value 0.9×10^{-76} (m^4/V)^2.[10] Assuming that all the vibrational modes of R−BN in the range 1300−1600 cm^{-1}, originating from CH

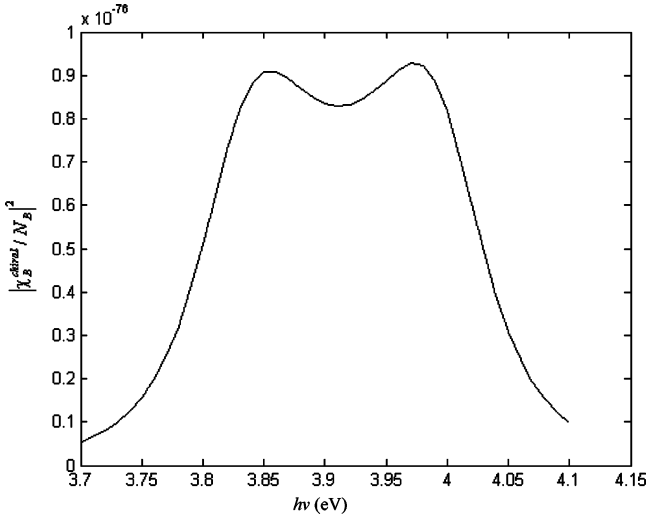

Figure 3. Calculated peak strengths of the chiral spectra $|\chi_B^{chiral}/N_B|^2$ ($(m^4/V)^2$) for vibrational mode of R−BN at 1383 A cm^{-1} versus the sum-frequency $h\upsilon$ around the resonance to the first two excited states based on ZINDO-1//AM1 computations with $\Delta_t = 0.1$

bending and ring deformation are of the same magnitude of the displacements, we take them to be 0.1 in the computation for simplification. In addition, we mention one detail about the chosen sum frequency υ in Figure 1. From eqs 4 and 5, we know that χ_B^{chiral} is determined by the difference ($\upsilon - \upsilon_{Mm,Gg}$) between the sum frequency and the excited energy, and not by either of them. In ref 10 the first excitonic resonance of BN is at 3.67 eV and the sum frequency is selected as 3.70 eV for an enhancement, hence in Figure 1 the SF is taken to be 0.03 eV larger than the first excited resonance 3.8276 eV calculated by ZINDO-1//AM1 computation (Table 2) for fitting to the experiment.

4.2. The Sum-Frequency Dispersion Spectra of BN Molecules. More detailed resonant enhancement behaviors of the 1383 A cm^{-1} vibrational modes are shown in Figure 3, where the peak strengths of the chiral spectra $|\chi_B^{chiral}/N_B|^2$ for this vibrational mode is computed and plotted against the sum-frequency $h\upsilon$ near the resonances to the first two singlet excited electronic states. It is shown that, in this sum-frequency dispersion spectra, there are doublet dispersion peaks with spacing 0.12 eV (968 cm^{-1}): one is at 3.86 eV and the other is 3.98 eV, which is in agreement with the experiment.[10] The splitting of the doublet dispersion peak is much larger than that of the first two excited electronic states (135 cm^{-1} by ZINDO-1//AM1, 29.8 cm^{-1} by TDDFT//B3LYP/6-31G*). The calculated result for 1383 A band in Table 4 show that, in the resonant-enhanced case, the peak strengths $|\chi_B^{chiral}/N_B|^2$ from the contribution of the second singlet excited electronic state is of the order of 10^{-104} $(m^4/V)^2$, which can be omitted when comparing with the contribution 10^{-76} $(m^4/V)^2$ from the first singlet excited electronic state. We find that there is no difference between the sum-frequency dispersion spectra if we only consider the first singlet excited electronic state. This indicates that due to the Franck−Condon progression in eqs 11 and 12 the doublet dispersion peaks in the IR−UV SFVS can be existent. The most striking evidence for the Franck−Condon progression nature of the doublet, which was demonstrated by Fischer et al.,[11] is that the electronic spectrum of BN indeed resembles that of 2-naphthol (2HN), and 2HN itself already exhibits a doublet.

TABLE 5: Computed Isotropic, Anisotropy, and Antisymmetric Placzek Invariants Σ^0, Σ^2, Σ^1 (in the unit of 1.0×10^{-80} $(C\cdot m^2/V)^2$), and the Depolarization Ratio ρ for Vibrational Modes of R−BN Marked in Figure 2 Based on ZINDO-1//AM1 Computations

band	Σ^0	Σ^1	Σ^2	I_{rel}	ρ
1318 B	0.00	0.13	0.01	0.024	31.4
1350 A	7.09	0.13	10.6	4.85	0.287
1383 A	6.63	1.41	9.84	4.74	0.346
1443 B	0.20	0.22	0.34	0.183	0.629
1455 A	4.91	0.40	6.71	3.27	0.291
1490 A	6.10	2.18	8.31	4.43	0.381
1540 B	0.05	0.18	0.03	0.054	1.65

5. Resonant Raman Spectra of R−BN Chiral Solution

According to eqs 11 and 12, based on ZINDO-1//AMI results and the foregoing parameters, we compute the fundamental frequencies, Placzek invariants (Σ^0,Σ^1, and Σ^2), relative intensity I_{rel}, and depolarization ratios of the vibrational bands in resonant Raman spectra of R−BN chiral solution. The calculated results are listed in Table 5. In the calculation, both Raman A and B terms from the resonances with the first two singlet excited states ^{1}B and ^{1}A are involved. In these computations, the sum-frequency is at 3.8076 eV and the displacement Δ_t is taken to be 0.1. In Table 5, Placzek invariants Σ^0,Σ^1, and Σ^2 are defined as[30] Thus Σ^0 is the isotropic part of the Raman tensor and Σ^2 is

$$\Sigma^0 = \frac{1}{3}|\alpha_{xx} + \alpha_{yy} + \alpha_{zz}|^2$$

$$\Sigma^1 = \frac{1}{2}\{|\alpha_{xy} - \alpha_{yx}|^2 + |\alpha_{xz} - \alpha_{zx}|^2 + |\alpha_{yz} - \alpha_{zy}|^2\}$$

$$\Sigma^2 = \frac{1}{2}\{|\alpha_{xy} + \alpha_{yx}|^2 + |\alpha_{xz} + \alpha_{zx}|^2 + |\alpha_{yz} + \alpha_{zy}|^2\} + \frac{1}{3}\{|\alpha_{xx} - \alpha_{yy}|^2 + |\alpha_{xx} - \alpha_{zz}|^2 + |\alpha_{yy} - \alpha_{zz}|^2\} \quad (19)$$

the symmetric anisotropy, while Σ^1 refers to the antisymmetric part of the tensor. Based on them, the total differential scattering cross-section ($d\sigma/d\Omega$) is

$$\left(\frac{d\sigma}{d\Omega}\right) = 4\pi^2\alpha^2\nu_s^4\left[\frac{1}{30}(10\Sigma^0 + 5\Sigma^1 + 7\Sigma^2)\right] \quad (20)$$

Thus the relative intensity I_{rel} in Table 5 may be chosen as

$$I_{rel} \propto \frac{1}{30}[(10\Sigma^0 + 5\Sigma^1 + 7\Sigma^2)] \quad (21)$$

Also the depolarization ρ described the polarization properties can be expressed into[30]

$$\rho = \frac{5\Sigma^1 + 3\Sigma^2}{10\Sigma^0 + 4\Sigma^2} \quad (22)$$

Comparing Table 5 with Table 1, the results indicate that (i) antisymmetric invariants Σ^1 in Table 5 are qualitatively proportional to the intensities of the corresponding vibration bands in IR−UV SFVS spectra, which is associated with eq 4 and supports the theory of SFVS.[7a,10] (ii) the qualitative agreement in positions and relative intensities of Raman vibration bands for the experimental and calculated spectra can be seen. Some quantitative differences between the experiment and calculated resonant Raman spectra might result from the different samples and conditions, where the experiment spectra are nonresonant

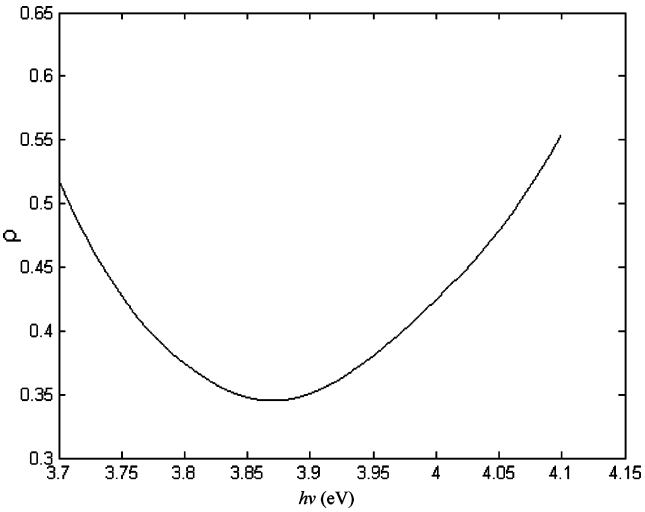

Figure 4. Calculated depolarization ratio ρ for vibrational mode of R−BN at 1383 A cm^{-1} versus the sum-frequency $h\nu$ based on ZINDO-1//AM1 computations.

Raman scattering of solid BN, the calculated spectra are resonant Raman scattering of a BN molecule.

We have also calculated the polarization dispersion curve for the 1383 A cm^{-1} band, i.e., the depolarization ratioρ for the vibrational mode at 1383 A cm^{-1} versus the sum-frequency $h\nu$ in the range of 3.7−4.1 eV, which is plotted in Figure 4. The prominent character of polarization dispersion curve in Figure 4 is the pronounced anti-resonance close to the sum-frequency resonance ~3.85 eV. Collins et al.[31] have reported polarization curves for A_2 modes of the haem proteins that show a pronounced anti-resonance close to the 0−0 band. Such an anti-resonance was explained as arising from electronic interference effect of approximate electronic degenerate states in cases where the distances between excited electronic states are of the same order of magnitude as the vibrational frequencies.[30] The anti-resonance of the polarization dispersion curve for the 1383 cm^{-1} band of BN reminds us of the similarity in antisymmetric Raman scattering between BN and metalloporphyrin molecules.[32] The anti-resonance phenomenon in Raman scattering was theoretically studied by the two-state model in ref 33.

6. Conclusions

The doubly resonant IR−UV sum-frequency vibrational spectroscopy (SFVS) of R-binaphthol solution is analyzed by expressing the corresponding nonlinear susceptibilities into the product of the antisymmetric part of the anti-Stokes Raman tensor and the vibrational transition moment. Then the A and B terms of Raman tensors and the vibrational transition moment are derived by using the Taylor expansion of the electronic transition moments with respect to the vibrational normal modes. Using the ZINDO-1//AM1 computations and the density functionals theory (BPW91/6-31G**, TD//B3LYP/6-31G*), we optimize and calculate IR frequencies, IR intensities, electronic excitation energies, and transition moments between the ground electronic state and the excited states for BN molecule. Based on the AM1/ZINDO calculations and the deduced formulas, the UV−IR doubly resonant SFVS for R−BN molecule is computed and assigned, the results indicate that for the most intense vibrational band observed in the SFVS experiment symmetry, frequencies, intensities, order and pattern of the enhanced vibrational modes agree with experiment qualitatively, and the studies for the corresponding resonant sum-frequency dispersion spectra indicate that due to the Franck−Condon progression, there are the doublet dispersion peaks. The polarization resonant Raman spectra for the vibrational modes appearing in SFVS of BN are also computed and associated with the experiment SFVS of BN. This direct evaluation of the Raman scattering tensors may provide a way of assigning the doubly resonant IR−UV SFVS, but so far only BN molecules have been investigated by the direct method, similar studies for more systems are needed.

Acknowledgment. This work was supported by the National Natural Science Foundation of China (grant no. 20473078) and the Development Foundation of the Education Department of China (grant no. 20020358061).

References and Notes

(1) Buckingham, A. D. *Optical, Electric and Magnetic Properties of Molecules−A Review of the Work of A. D. Buckingham;* Clary, D. C., Orr, B. J., Eds.; Elsevier: Amsterdam, 1997.
(2) Barron, L. D. *Molecular Light Scattering and Optical Activity;* Cambridge University Press: Cambridge, 1982.
(3) Barron, L. D.; Buckingham, A. D. *Acc. Chem. Res.* **2001**, *34*, 781.
(4) Spiro, T. G.; Stein, P. *Annu. Rev. Phys. Chem.* **1977**, *28*, 501.
(5) Zheng, R.-H.; Chen, D.-M.; Wei, W.-M.; He, T.-J.; Liu, F.-C. *J. Chem. Phys.* **2004**, *121*, 6835.
(6) Zheng, R.-H.; Chen, D.-M.; He, T.-J.; Liu, F.-C. *Chem. Phys.* **2002**, *285*, 261.
(7) (a) Fischer, P.; Wiersma, D. S.; Righini, R.; Champagne, B.; Buckingham, A. D. *Phys. Rev. Lett.* **2000**, *85*, 4253. (b) Fischer, P.; Buckingham, A. D.; Albrecht, A. C. *Phys. Rev. A* **2001**, *64*, 053816.
(8) (a) Belkin, M. A.; Kulakov, T. A.; Ernst, K. H.; Yan, L.; Shen, Y. R. *Phys. Rev. Lett.* **2000**, *85*, 4474. (b) Belkin, M. A.; Shen, Y. R. *Int. Rev. Phys. Rev.* **2005**, *24*, 257.
(9) Belkin, M. A.; Han, S.-H.; Wei, X.; Shen, Y. R. *Phys. Rev. Lett.* **2001**, *87*, 113001.
(10) Belkin, M. A.; Shen, Y. R. *Phys. Rev. Lett.* **2003**, *91*, 213907.
(11) Fischer, P.; Wise, F. W.; Albrecht, A. C. *J. Phys. Chem. A* **2003**, *107*, 8232.
(12) Hayashi, M.; Lin, S. H.; Shen, Y. R. *J. Phys. Chem. A* **2004**, *108*, 8058.
(13) Belkin, M. A.; Shen, Y. R.; Harris, R. A. *J. Chem. Phys.* **2004**, *120*, 10118.
(14) Moad, A. J.; Simpson, G. J. *J. Phys. Chem. B* **2004**, *108*, 3548.
(15) Byers, J. D.; Hicks, J. M. *Chem. Phys. Lett.* **1994**, *231*, 216.
(16) Nogueira, H. I. S.; Quintal, S. M. O. *Spectrochimica Acta A* **2000**, *56*, 959.
(17) Setnička, V.; Urbanová, M.; Bouř, P.; Král, V.; Volka, K. *J. Phys. Chem. A* **2001**, *105*, 8931.
(18) Warshel, A.; Dauber, P. *J. Chem. Phys.* **1977**, *66*, 5477.
(19) Warshel, A *Annu. Rev. Biophys. Bioeng.* **1977**, *6*, 273.
(20) Shen, Y. R. *Annu. Rev. Phys. Chem.* **1989**, *40*, 327.
(21) Shen, Y. R. Chapter 2. In *The Principles of Nonlinear Optics;* Wiley: New York, 1984.
(22) Warshel, A. *Chem. Phys. Lett.* **1976**, *43*, 273.
(23) Liu, F.-C. *J. Phys. Chem.* **1991**, *95*, 7180.
(24) Liu, F.-C.; Buckingham, A. D. *Chem. Phys. Lett.* **1993**, *207*, 325.
(25) Komornicki, A.; Jaffe, R. L. *J. Chem. Phys.* **1979**, *71*, 2150.
(26) Frisch, M. J.; Trucks, G. W.; Schlegel, H. B.; Scuseria, G. E.; Robb, M. A.; Cheeseman, J. R.; Zakrzewski, V. G.; Montgomery, J. A., Jr.; Stratmann, R. E.; Burant, J. C.; Dapprich, S.; Millam, J. M.; Daniels, A. D.; Kudin, K. N.; Strain, M. C.; Farkas, O.; Tomasi, J.; Barone, V.; Cossi, M.; Cammi, R.; Mennucci, B.; Pomelli, C.; Adamo, C.; Clifford, S.; Ochterski, J.; Petersson, G. A.; Ayala, P. Y.; Cui, Q.; Morokuma, K.; Malick, D. K.; Rabuck, A. D.; Raghavachari, K.; Foresman, J. B.; Cioslowski, J.; Ortiz, J. V.; Stefanov, B. B.; Liu, G.; Liashenko, A.; Piskorz, P.; Komaromi, I.; Gomperts, R.; Martin, R. L.; Fox, D. J.; Keith, T.; Al-Laham, M. A.; Peng, C. Y.; Nanayakkara, A.; Gonzalez, C.; Challacombe, M.; Gill, P. M. W.; Johnson, B. G.; Chen, W.; Wong, M. W.; Andres, J. L.; Head-Gordon, M.; Replogle, E. S.; Pople, J. A. *Gaussian 98*, revision A.11; Gaussian, Inc.: Pittsburgh, PA, 1998.
(27) Scott, A. P.; Radom, L. *J. Phys. Chem.* **1996**, *100*, 16502.
(28) Manneback, C. *Physica* **1951**, *11*, 1001.
(29) Kanis, D. R.; Ratner, M. A.; Marks, T. J. *Chem. Rev.* **1994**, *94*, 195.
(30) Mortensen, O. S.; Hassing, S. *Adv. Infrared Raman Spectrosc.* **1980**, *6*, 1.
(31) Collins, D. W.; Champion, P. M.; Fitchen, D. B. *Chem. Phys. Lett.* **1976**, *40*, 416.
(32) Xie, R.; Chen, D.-M.; He, T.-J.; Liu, F.-C. *J. Phys. Chem. A* **2004**, *108*, 4491.
(33) Hassing, S. *J. Raman Spectrosc.* **1997**, *28*, 739.